processes

MDPI

Review

Driving Sustainable Energy Co-Production: Gas Transfer and Pressure Dynamics Regulating Hydrogen and Carboxylic Acid Generation in Anaerobic Systems

Xiao Xiao, Meng He, Yanning Hou, Bilal Abdullahi Shuaibu, Wenjian Dong, Chao Liu and Binghua Yan *

College of Environment and Ecology, Hunan Agricultural University, Changsha 410128, China; xiao_xiao0426@126.com (X.X.); hemeng202202@163.com (M.H.); hyn15200800613@163.com (Y.H.); kirareshuaibu@gmail.com (B.A.S.); wjdong0204@163.com (W.D.); liuchao@hunau.edu.cn (C.L.)
* Correspondence: binghuayan@hunau.edu.cn; Tel.: +86-15265293850

Abstract

To achieve energy transition, hydrogen and carboxylic acids have attracted much attention due to their cleanliness and renewability. Anaerobic fermentation technology is an effective combination of waste biomass resource utilization and renewable energy development. Therefore, the utilization of anaerobic fermentation technology is expected to achieve efficient co-production of hydrogen and carboxylic acids. However, this process is fundamentally affected by gas–liquid mass transfer kinetics, bubble behaviors, and system partial pressure. Moreover, the related studies are few and unfocused, and no systematic research has been developed yet. This review systematically summarizes and discusses the basic mathematical models used for gas–liquid mass transfer kinetics, the relationship between gas solubility and mass transfer, and the liquid-phase product composition. The review analyzes the roles of the headspace gas composition and partial pressure of the reaction system in regulating co-production. Additionally, we discuss strategies to optimize the metabolic pathways by modulating the gas composition and partial pressure. Finally, the feasibility of and prospects for the realization of hydrogen and carboxylic acid co-production in anaerobic fermentation systems are outlined. By exploring information related to gas mass transfer and system pressure, this review will surely provide an important reference for promoting cleaner production of sustainable energy.

Keywords: hydrogen and carboxylic acid co-production; sustainable energy sources; gas–liquid mass transfer; gas partial pressure; regulation

check for updates

Academic Editor: Davide Papurello

Received: 3 July 2025
Revised: 18 July 2025
Accepted: 21 July 2025
Published: 23 July 2025

Citation: Xiao, X.; He, M.; Hou, Y.; Shuaibu, B.A.; Dong, W.; Liu, C.; Yan, B. Driving Sustainable Energy Co-Production: Gas Transfer and Pressure Dynamics Regulating Hydrogen and Carboxylic Acid Generation in Anaerobic Systems. *Processes* **2025**, *13*, 2343. https://doi.org/10.3390/pr13082343

Copyright: © 2025 by the authors. Licensee MDPI, Basel, Switzerland. This article is an open access article distributed under the terms and conditions of the Creative Commons Attribution (CC BY) license (https://creativecommons.org/licenses/by/4.0/).

1. Introduction

Global economic advancement has triggered unprecedented energy consumption [1,2], driving both energy security concerns and environmental problems [3]. Despite shifts toward renewables, fossil resources retain dominance within the current energy portfolio [4], with their annual utilization continuing to rise [5]. The finite nature of these fuels, compounded by excessive exploitation, intensifies resource scarcity. Furthermore, pollutants, e.g., CO_2, SO_2, and NO_x, primarily drive critical environmental challenges such as global warming, photochemical smog, and haze formation [6]. Accelerating this energy transition, numerous nations have recently committed to "carbon neutrality" or "zero carbon" climate objectives, enacting supportive policies [7]. Among sustainable alternatives, hydrogen and carboxylic acids (e.g., acetic acid, butyric acid) represent promising candidates owing to their high energy density and low environmental impact [8].

Carboxylic acids, obtained through fermentation or thermochemical conversion of biomass, serve as versatile platform molecules that can be efficiently upgraded into valuable liquid biofuels (like biodiesel precursors) and biochemicals, offering crucial solutions for replacing fossil-derived liquid fuels and enabling carbon recycling [9]. Hydrogen, on the other hand, stands out as a premier clean energy carrier for the future due to its exceptionally high energy density (per mass), zero direct carbon emissions at the point of use, and versatility in applications ranging from fuel cells to industrial processes [10]. In conclusion, both pathway—the valorization of biomass-derived carboxylic acids and the utilization of clean hydrogen—are critical and complementary strategies for achieving deep decarbonization and energy security.

Conventional synthesis processes for carboxylic acids (e.g., acetic acid via methanol carbonylation [11], butyric acid via propylene carbonylation [12]) and hydrogen production technologies (e.g., coal gasification [13], natural gas reforming [14]) exhibit heavy reliance on fossil feedstocks. While demonstrating advantages in process maturity and cost-effectiveness, these methods incur significant environmental burdens due to their high carbon emission intensity and energy-intensive operations [15–17]. Against the dual pressures of escalating environmental concerns and surging demand for green chemicals, developing efficient and clean co-production technologies for carboxylic acids and hydrogen has become critically imperative.

Within the multiphase reactions of anaerobic fermentation (AF), the acidogenic phase and hydrogen-producing acetogenic stage are intrinsically interlinked. Acidogenic fermentative bacteria initially hydrolyze and acidify complex organic compounds into small-molecule organic acids such as acetate, butyrate, and propionate, providing essential substrates for subsequent hydrogen-producing acetogens. Hydrogen-producing acetogens then metabolize these organic acids to generate hydrogen, acetate, and carbon dioxide, thereby achieving biological hydrogen production [18]. Certain microorganisms exhibit dual functionality under specific conditions, participating in both acidogenesis and hydrogen production [19]. For example, some acidogenic bacteria decompose organics into organic acids via fermentation in anaerobic environments. When environmental conditions become favorable, these organic acids can be further utilized by hydrogenogens to produce hydrogen. Butyrate-type fermentative bacteria exemplify this mechanism: they produce butyrate, acetate, and other organic acids during acidogenesis, which subsequently serve as substrates for hydrogenogens to metabolically generate hydrogen [17]. Propionic acid-producing bacteria utilize H_2 to convert glucose into propionic acid and CO_2 [20]. From this, in the process of anaerobic fermentation for acid production, different types of microbial activities are often accompanied by the production and consumption of a large amount of by-product gases, mainly H_2 and CO_2, which can account for 30% of the consumed substrates [21]. The dissolved H_2/CO_2 content in the fermentation broth is usually in an interactive regulation state with the headspace H_2/CO_2 partial pressure, that is, the dissolved H_2/CO_2 concentration is positively correlated with the partial pressure, thereby affecting the gas–liquid mass transfer efficiency of the reaction system. Therefore, headspace pressure and gas partial pressure are key factors affecting the type of acid metabolism and product recovery efficiency. However, the current theory on gas–liquid mass transfer regulation for anaerobic fermentation of hydrogen and carboxylic acid co production is not systematic enough.

Compared to alternative technologies, AF demonstrates advantages including broad substrate adaptability, operational simplicity, and significant application potential, rendering it more feasible for industrial implementation [22]. This technology utilizes waste biomass (e.g., industrial residues, municipal solid waste, wastewater, food waste) as feedstocks, effectively integrating waste valorization with renewable energy development [23].

Consequently, AF represents the most promising approach for co-producing carboxylic acids and hydrogen. However, significant challenges persist in regulating the H_2 and carboxylic acid co-production process. Key unresolved issues include developing effective control measures to alleviate product inhibition [24], optimizing reactor configuration to improve gas–liquid mass transfer efficiency [25], and integrating supplementary methods to enhance microbial electron transfer efficiency [26]. Furthermore, the abovementioned research content is scattered and the evaluation criteria are not unified, which greatly hinders the retrieval, comparison of effects, and even technological progress of related research.

To clarify the co-production process of hydrogen and carboxylic acids via AF, along with the underlying principles and technologies for its regulation, this review first outlines the relevant microbial metabolic pathways. Subsequently, the impact mechanisms of headspace gas partial pressure and gas–liquid mass transfer efficiency on co-production are discussed, analyzed from the perspectives of both the reactor headspace and the fermentation broth. Finally, strategies and prevailing techniques for enhancing the yield of hydrogen and carboxylic acid co-production are summarized. We examine the critical role of gas–liquid mass transfer efficiency in anaerobic dark fermentation systems for hydrogen and carboxylic acid co-production and construct a circular economy model with dual environmental and economic benefits.

2. Biological Metabolism of Anaerobic Co-Production of Carboxylic Acids and Hydrogen

AF facilitates the co-production of hydrogen and organic carboxylic acids through a complex biological mechanism. This process relies on microbial metabolism to transform organic substrates into both H_2 and valuable carboxylic acids [27]. As shown in Figure 1, organic matter introduced into the AF system undergoes sequential degradation via three key stages: hydrolysis, fermentation, and acetogenesis.

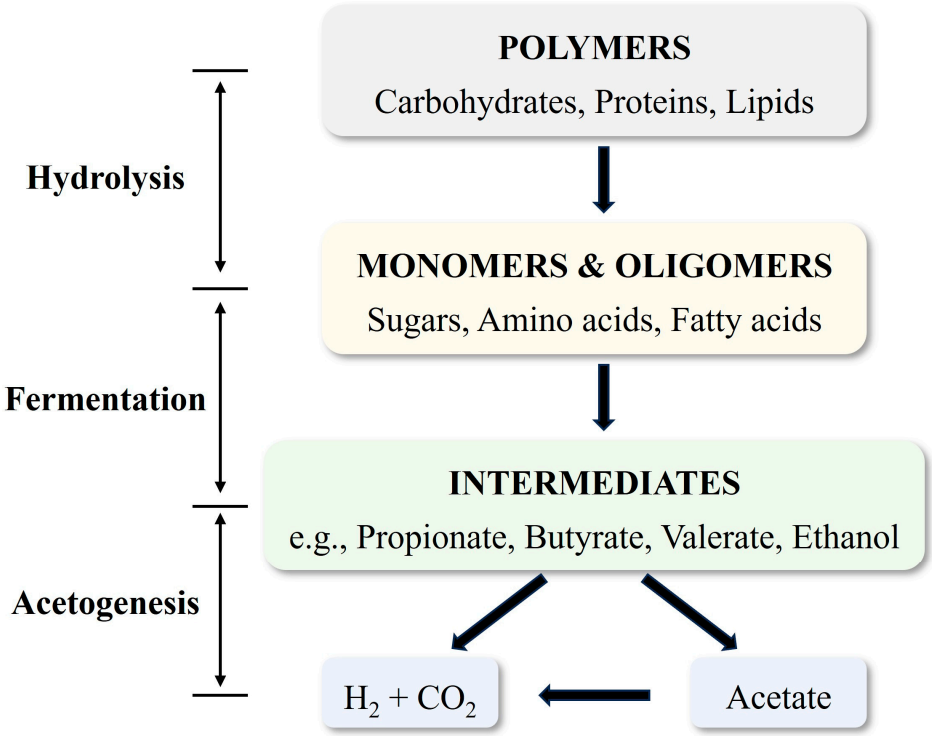


Figure 1. Flowchart of anaerobic co-production of carboxylic acids and hydrogen. Adapted from [27].

Within this mechanism, protons (H^+) serve as terminal electron acceptors. They neutralize electrons released during microbial substrate oxidation, culminating in hydrogen

production (Equation (1)) [28]. Generally, the AF initiates with carbohydrate catabolism (Figure 2). Carbohydrates undergo enzymatic hydrolysis to yield glucose as the primary soluble monomer. Subsequently, through the process of glycolysis, glucose breaks down into pyruvate, while adenine dinucleotide ion (NAD^+) is reduced to nicotinamide adenine dinucleotide (NADH), accompanied by H^+ generation (Equation (2)) [29]. The metabolism of pyruvate mainly involves conversion to acetyl coenzyme A (acetyl-CoA), CO_2, and H_2 via the pyruvate formate lyase (PFL) pathway, pyruvate ferredoxin oxidoreductase (PFOR) pathway, and NADH reoxidation (Equations (3)–(7)) [30]. The PFOR and NADH reoxidation pathways are prevalent among strictly anaerobic bacteria.

$$2H^+ + 2e^- \leftrightarrow H_2 \quad (1)$$

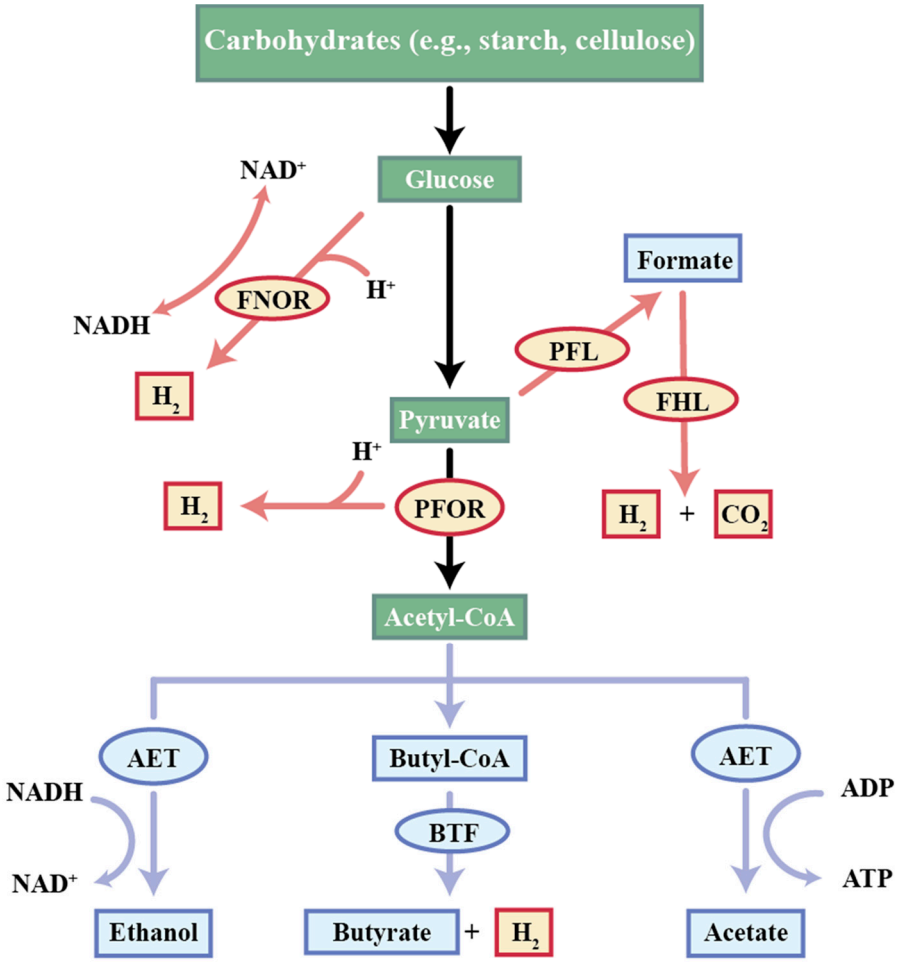


Figure 2. Metabolic pathways of anaerobic co-production of carboxylic acids and hydrogen. Abbreviations: NAD^+: adenine dinucleotide ion; NADH: nicotinamide adenine dinucleotide; Acetyl-CoA: acetyl coenzyme A; PFL: pyruvate formate lyase; PFOR: pyruvate ferredoxin oxidoreductase; FNOR: ferredoxin-dependent $NADP^+$ oxidoreductase; FHL: formate hydrogen lyase; AET: acetate–ethanol-type fermentation; BTF: butyrate fermentation; ATP: adenosine triphosphate; ADP: adenosine diphosphate.

Glycolysis:

$$C_6H_{12}O_6 + 2NAD^+ \rightarrow 2CH_3COCOOH + 2NADH + 2H^+ \quad (2)$$

Pyruvate formate lyase (PFL pathway):

$$2C_3H_4O_3 + 2H\text{-}CoA \rightarrow 2Acetyl\text{-}CoA + 2CH_2O_2 \quad (3)$$

$$2CH_2O_2 \rightarrow 2H_2 + 2CO_2 \quad (4)$$

Pyruvate ferredoxin oxidoreductase (PFOR pathway):

$$CH_3COCOOH + CoA + 2Fd_{ox} \rightarrow acetyl\text{-}CoA + 2Fd_{red} + CO_2 \quad (5)$$

$$Fd_{red} + 2H^+ \rightarrow Fd_{ox} + H_2 \quad (6)$$

Additional H_2 formation:

$$NADH + H^+ \rightarrow H_2 + NAD^+ \quad (7)$$

These metabolic pathways drive the synthesis of carboxylic acids. Downstream of pyruvate, acetyl-CoA serves as the pivotal branch point determining the type and yield of acids [18]. The co-production of H_2 and carboxylic acids via anaerobic fermentation (AF) is categorized into three primary types based on dominant end metabolites: butyrate fermentation (BTF), propionate fermentation (PPF), and acetate–ethanol-type fermentation (AET) [31,32]. Studies indicate that varying environmental conditions select for distinct microbial consortia within the system, thereby determining the prevailing fermentation pathway [31].

- Butyrate Fermentation

The butyrate fermentation pathway is primarily mediated by strictly or facultatively anaerobic bacteria, with *Clostridium* spp. constituting the dominant genus. BTF yields butyrate and acetate as primary metabolites, typically generating significant H_2. Following glucose conversion to acetyl-CoA, this intermediate is transformed into butyryl-CoA. Subsequently, phosphotransbutyrylase (PTB) and butyrate kinase (BK) catalyze the sequential conversion of butyryl-CoA to butyryl phosphate and finally butyrate. In this process, Fd_{red} transfers electrons to hydrogenase, which reduces protons (H^+) to generate H_2 [33].

- Propionate Fermentation

Unlike butyrate production pathways, propionate generation exhibits high reducing power, facilitating NADH oxidation. During anaerobic digestion of organic wastes, acidogenic degradation frequently occurs via this fermentation type. *Propionibacterium* spp. serve as the primary metabolic drivers. Key liquid metabolites include propionic and acetic acids, though minimal gas production occurs since propionibacteria generally lack hydrogenase enzymes [34].

- Acetate-Ethanol Fermentation

Dominant ethanol-fermenting genera include Bacteroides, Pseudomonas fermentans, Fusobacteria, Bacteroides, and Clostridium. This pathway primarily yields ethanol and acetate as end metabolites. Like BTF and PPF, ethanol fermentation also generates substantial H_2 and efficiently oxidizes NADH. Critically, acetate synthesis enables regeneration of 4 mol NAD^+ per mole glucose oxidized. Compared to BTF, this represents a doubling of NAD^+ production. The AET exhibits robust NADH–NAD^+ balancing capability. Consequently, AET generally demonstrates superior process stability and higher H_2 yields compared to BTF [35]. Details regarding the co-production of hydrogen and carboxylic acids through anaerobic fermentation are presented in Table 1.

While low concentrations of the production can enhance co-production of H_2 and carboxylic acids, elevated levels acidify the system and suppress both production rates

and yields. During acid accumulation, these metabolic by-products lower extracellular pH. Critically, both dissociated (anionic) and undissociated (protonated) acid forms inhibit acidogenesis [36]. Dissociated acids increase medium ionic strength through acid-producing bacteria (APB) cell lysis [37], impairing H_2 generation and triggering a metabolic shift from acidogenesis to solventogenesis [36]. Undissociated acids diffuse across cell membranes into higher-pH cytoplasm, where they dissociate and release protons [36]. This intracellular proton influx can disrupt cytoplasmic pH homeostasis, inhibit core metabolic enzymes, and cause cell mortality and suppresses H_2/carboxylate co-production [38,39]. In addition, ATP-dependent proton extrusion consumes cellular energy reserves [39], depleting ATP otherwise available for growth and biosynthesis.

H_2 exhibits inherently low aqueous solubility [2]. H_2 supersaturation in fermentative reactors typically stems from inadequate gas–liquid mass transfer [40]. Critically, accumulated dissolved H_2 suppresses hydrogenase activity and acidogenesis [41] while concurrently redirecting metabolic flux toward alternative products like lactate, ethanol, acetone, and butanol [42]. Therefore, dissolved H_2 accumulation may inhibit microbial growth kinetics and reduce H_2 and carboxylic acid co-productivity.

Table 1. Products and yields in AF for hydrogen and carboxylic acid co-production.

Substrate	Operating Conditions	Key Microorganism	Main Metabolites	Co-Production Yield	Ref.
Waste activated sludge	With 90 mg/g VSS urea at a constant pH of 9.5	*Acinetobacter*, *Tissierella*, and *Petrimonas*	H_2, acetic and butyric acid	24.57 mL/g VSS of H_2 and 72.80 mg COD/g VSS of SCFAs.	[43]
Food waste	Control pH at 7	*Clostridium_sensu_stricto_1*	H_2, acetic and butyric acid	21.49 L/L of H_2 and the production of butyrate increased to 42.13 g/L.	[44]
Food waste	Add 3 g/L lactic acid	*Clostridium_sensu_stricto_12*	H_2 and butyric acid	57.02 ± 2.10 mL/g VSS of H_2	[45]
Melon and watermelon	A high HRT of 27 d, an organic loading rate of 3 g of VS per day	*Ruminococcus*	H_2, iso-butyric, and caproic acids	395.5 mL/g VS of H_2, the content of iso-butyric and hexanoic acid can reach 76% of the SCFAs	[46]
Food waste	Add 8% oyster shells (*w*/*w*)	*Lactobacillales*, *Gallicola*, and *Bacteroides*	H_2, acetic and butyric acid	88.2 mL/g VS of H_2, the highest concentrations of butyric and acetic acid can reach 8048.4 mg/L and 5604.6 mg/L, respectively.	[47]
Food waste	Add different levels of tar and BES	*Clostridium_sensu_stricto* and *Clostridium_IV*	H_2, butyric and caproic acids	65.0 mL/g VS of H_2 (with a tar addition of 5 g/L), and the cumulative butyric acid production can reach 726.8 mg COD/g VS (with a tar addition of 30 g/L).	[48]

3. Gas–Liquid Mass Transfer in Co-Production of Carboxylic Acids and Hydrogen

3.1. System Pressure in Co-Production of Carboxylic Acids and Hydrogen

Anaerobic acidogenic fermentation generates substantial gaseous by-products, predominantly H_2 and CO_2, existing as bubbles in the fermentation broth and as headspace gas. These significantly influence the thermodynamic spontaneity and reaction directionality of associated metabolic processes. While headspace composition shows no direct correlation with hydrogen production under certain conditions [40], headspace pressure remains a decisive factor for carboxylic acid and H_2 co-production efficiency [49]. Consequently,

reducing H_2 partial pressure in the headspace serves as a validated strategy to enhance co-product yields [50].

$$C_6H_{12}O_6 + 2H_2O \rightarrow 2C_2H_4O_2 + 2CO_2 + 4H_2\ \Delta G = -133.44\ \text{kJ/mol} \quad (8)$$

Le Chatelier's principle (Equation (8)) dictates that by in situ removal of H_2 (e.g., by reducing its partial pressure), the product inhibitory effect can be alleviated and thermodynamic circumstances improved, hence promoting the metabolic route for hydrogen synthesis. This thermodynamically favors enhanced carboxylic acid and hydrogen yields through Gibbs free energy minimization.

Acidogenic bacteria exhibit significant metabolic sensitivity to hydrogen partial pressure ($P(H_2)$). As governed by Henry's law (Equation (9)), $P(H_2)$ in the gas phase directly regulates dissolved H_2 concentrations in fermentation broth. To optimize carboxylic acids and H_2 co-production, dissolved H_2 accumulation must be minimized through active $P(H_2)$ reduction strategies.

$$K_H^i = \frac{P_G^i}{C_F^i} \quad (9)$$

K_H^i = Henry's constant for gas i ($m^3 \cdot Pa \cdot mol^{-1}$).
P_G^i = Partial pressure of gas i in the gas phase (Pa).
C_F^i = Dissolved concentration of gas i in the liquid phase ($mol \cdot m^{-3}$).

It is worth noting that Henry's law is applicable solely when the molecular state of the solute is identical in both the gas and liquid phases.

It is reported that the energy distribution of biochemical reactions is affected by hydrogen pressure. The reaction proceeds smoothly only when the H_2 partial pressure is $<6 \times 10^{-4}$ atm. Otherwise, its thermodynamic feasibility is limited. Elevated hydrogen partial pressure thermodynamically inhibits the degradation of propionate and certain amino acids by reducing reaction favorability ($\Delta G > 0$). Moreover, it disrupts the NADH–NAD^+ redox balance, suppressing hydrogenase activity and impairing hydrogenogenic metabolism [51]. In another study, elevated hydrogen partial pressure induced a metabolic shift from mixed-acid fermentation pathways (dominated by acetic acid and butyric acid production) toward solventogenic fermentation pathways characterized by reductive product formation (such as alcohols) [52]. Consequently, maintaining an appropriate $P(H_2)$ helps preserve the activity of the acidogenesis pathway, mitigates dissolved H_2 inhibition, and optimizes the co-production of H_2 and carboxylic acids.

3.2. Mass Transfer Characteristic in Anaerobic Fermentation

In AF systems, headspace hydrogen partial pressure $P(H_2)$ is the preferred monitoring parameter due to practical measurement feasibility via pressure sensors and gas chromatography. As established, elevated $P(H_2)$ disrupts metabolic pathways, destabilizing carboxylic acid and hydrogen yields. Critically, dissolved hydrogen accumulation exerts direct biological inhibition, and increasing liquid-phase H_2 concentration suppresses co-production efficiency through dual-phase feedback [50,53]. While Henry's law (Equation (9)) defines an equilibrium relationship between headspace $P(H_2)$ and dissolved H_2 concentration, mass transfer limitations in AF reactors prevent this equilibrium from being practically achieved. Consequently, Henry's Law becomes inadequate for AF systems. Empirical studies under three different controlled total pressure conditions demonstrate that H_2 and carboxylic acid co-production correlates directly with dissolved H_2 concentration, not headspace $P(H_2)$. This evidence establishes dissolved H_2 concentration as the definitive control parameter for optimizing AF performance [54]. Although dissolved hydrogen is frequently presumed to be at gas–liquid equilibrium [55], dissolved H_2 frequently enters

supersaturated states in AF systems. When microbial hydrogen production rates exceed the gas–liquid mass transfer capacity, dissolved H_2 accumulates to concentrations three to eight times higher than Henry's law predictions (Equation (9)) [41]. This supersaturated state thermodynamically constrains both carboxylic acid synthesis and hydrogen evolution [56]. Productivity remains constrained until dynamic equilibrium for H_2 production rates with mass transfer capacity is restored [55]. Elevated dissolved hydrogen concentrations additionally drive detrimental shifts in microbial consortia, further suppressing carboxylic acid and hydrogen yields [57]. Fundamentally, near-stoichiometric yields require near-equilibrium dissolved H_2 conditions, achievable only through impractically low production rates or ultralow-headspace $P(H_2)$. Therefore, dissolved H_2 concentration serve as the primary inhibition metric for carboxylic acid and hydrogen co-production systems [58]. Contemporary hydrogen monitoring in AF systems relies predominantly on liquid-phase sensors capable of detecting dissolved H_2 partial pressure. Such sensors need to have high sensitivity and selectivity and must be able to withstand the harsh environment within AF systems, including corrosivity, temperature variations, and pH changes. Nevertheless, current liquid-phase hydrogen sensors remain technologically immature for widespread deployment in AF systems.

Fundamental theories of interphase mass transfer (gas–liquid/liquid–gas) in biological systems are well established in the chemical engineering literature. AF represents a complex gas–liquid–solid three-phase system where hydrogen transfer from liquid to gas phase critically governs process efficiency. Optimized mass transfer conditions enable equilibrium between substrate supply and product expulsion during microbial metabolism, preventing the accumulation of reductive metabolites. This facilitates enhanced yield and compositional stability of acidogenic products such as carboxylic acids and hydrogen. Gaseous metabolites (e.g., H_2, CO_2) nucleate within the liquid phase and undergo phase transfer driven by concentration gradients. The primary mass transfer resistance occurs at gas–liquid interfaces, specifically within the hydrodynamic boundary layer, a zone of stagnant flow. This interfacial resistance impairs dissolved gas flux to the headspace [40]. Elevated dissolved hydrogen partial pressure within the liquid phase is a critical factor inhibiting anaerobic acidogenic fermentation [49]. To mitigate this inhibition, generated hydrogen must not only transfer from the liquid to the gas phase but also be actively removed from the system headspace. While releasing accumulated gas from the headspace is operationally straightforward, optimizing the interphase mass transfer of hydrogen between the liquid and gas phases represents the fundamental challenge for sustaining low dissolved H_2 levels and headspace pressure stability. Figure 3 illustrates the key gas–liquid mass transfer pathways and resistances relevant to hydrogen dynamics in such an anaerobic fermentation system.

In mass transfer processes, the mass transfer coefficient quantifies the process's intrinsic enhancement potential. It represents the solute flux (mass transferred per unit time and unit interfacial area) occurring under a unit concentration or partial pressure difference driving force. The defining relationship for the mass transfer coefficient is given by Equation (10).

$$N_A = k(C_{Ai} - C_A) \quad (10)$$

N_A = Mass transfer flux ($mol \cdot s^{-1} \cdot m^2$).

k = Mass transfer coefficient ($m \cdot s^{-1}$).

$C_{Ai} - C_A$ = Concentration difference between the two phases ($mol \cdot m^3$).

The form of the mass transfer coefficient depends on the specific system (e.g., gas–liquid, liquid–solid) and the choice of driving force (e.g., concentration, partial pressure, mole fraction).

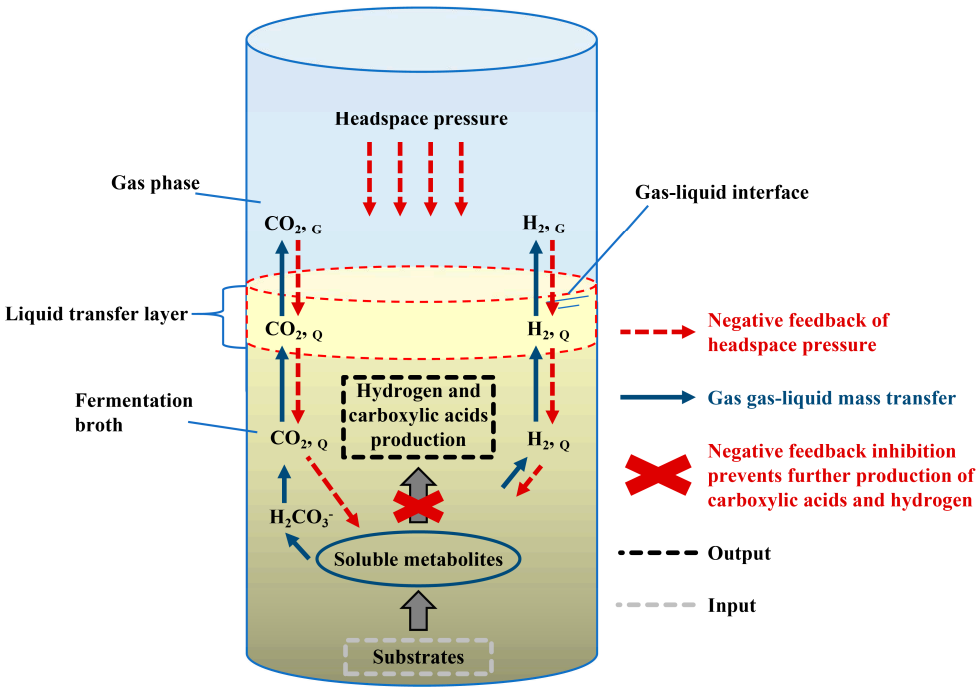


Figure 3. Mass transfer of gases in carboxylic acids and hydrogen co-production systems. Adapted from [40]. Abbreviations: G: gas phase; Q: liquid phase.

Beyond the mass transfer coefficient, mass transfer efficiency provides an alternative metric for characterizing interphase transport. This efficiency parameter is particularly prevalent in polymer devolatilization, where devolatilization efficiency quantifies the mass transfer performance of the process. Assuming negligible density and volume changes during mass transfer, devolatilization efficiency is defined by the following expression (Equation (11)).

$$E_f = \frac{C_0 - C_{av}}{C_0 - C_e} \tag{11}$$

C_0 = Initial concentration of substances (mol·m^{-3}).
C_{av} = Concentration of substances at the gas–liquid interface (mol·m^{-3}).
C_e = Equilibrium concentration of substances in the gas–liquid phase (mol·m^{-3}).
E_f = Mass transfer efficiency.

This represents the fractional approach to thermodynamic equilibrium, quantifying the proportion of maximum possible transfer achieved. Equation (12) describes the short-lived regime.

$$\frac{E_f}{t} = K_L a \tag{12}$$

E_f = Mass transfer efficiency.
t = Mass transfer time (s).
K_L = Liquid-side mass transfer coefficient (m·s^{-1}).
a = Interface area (m^2·m^{-3}).

In industrial practice, the foam-enhanced gas–liquid interface makes direct measurement of a exceptionally challenging. Consequently, $K_L a$ is operationally treated as a lumped parameter (volumetric mass transfer coefficient) with units (s^{-1}).

By classical definition, $K_L a$ represents the global volumetric mass transfer coefficient [41]. This lumped parameter quantifies gas–liquid interfacial transfer capacity in bioreactors (Equation (13)). Its operational dominance stems from the immeasurability of the true

interfacial area (a) in multiphase systems, hydrodynamic coupling of K_La and a, and direct experimental determination via dynamic methods.

$$Q = K_La \cdot He^{-1} \cdot \left(P_G - P_G^{\circ}\right) \quad (13)$$

Q = Molar gas transfer rate ($mol \cdot s^{-1}$).

K_La = Volumetric mass transfer coefficient (s^{-1}) (dependent on mixing intensity and interfacial area).

P_G = Partial pressure in the gas phase (Pa).

P_G° = Equilibrium partial pressure (Pa).

H = Henry's constant ($Pa \cdot m^3 \cdot mol^{-1}$).

H is exclusively an intrinsic property of the gas compound, independently of bioreactor conditions or biological factors [54]. The volumetric mass transfer coefficient (K_La) is indeed an appropriate efficiency metric for biohydrogen systems, as substantiated by experimental studies [41]. Accurately quantifying the volumetric mass transfer coefficient (K_La) in real time remains challenging. Furthermore, mass transfer dynamics within anaerobic acidogenic fermentation systems are insufficiently investigated, representing a significant research gap. This limitation is particularly critical, as mass transfer constraints are pervasive in bioreactor operation. Resolving these complex, multifactorial mass transfer issues continues to pose substantial difficulties for which satisfactory solutions are still lacking.

3.3. Key Determinants of Interfacial Transport

Key factors governing mass transfer encompass: (1) operational parameters (temperature, pressure, pH), (2) physicochemical characteristics of fermentation broth (viscosity, composition, rheology, inhibitory metabolites), and (3) bioreactor design (configuration, geometric parameters, agitation regimes) [59]. Figure 4 schematizes these gas–liquid transfer determinants in anaerobic fermentation systems.

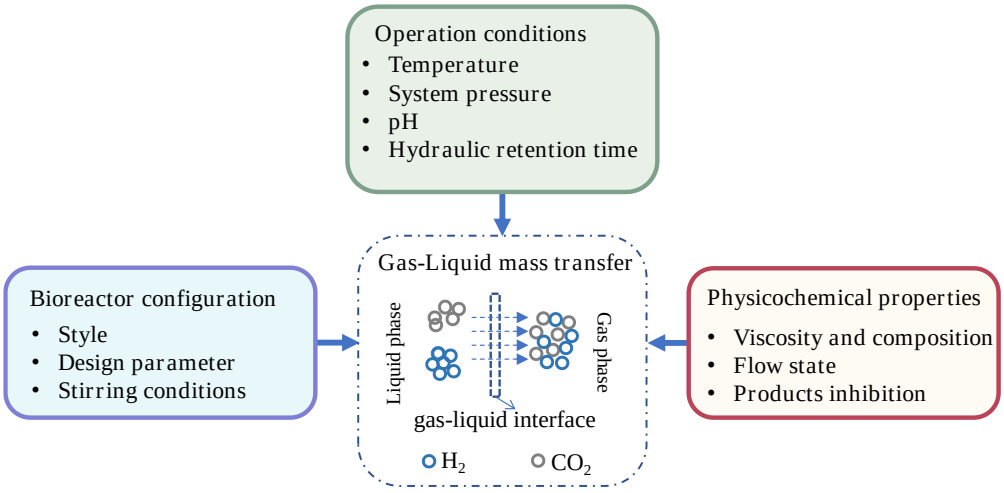


Figure 4. The influencing factors of mass transfer.

Temperature and pressure modulate both fermentation broth properties and microbial kinetics, thereby governing mass transfer efficiency [31]. In Sieborg's study [60], a model was established to examine the effect of temperature on the mass transfer rate of H_2 between gas and liquid phases. The results indicated that as the temperature increased to 65.4 °C, the mass transfer rate showed an upward trend. However, beyond this temperature, the mass transfer driving force was severely weakened due to the decrease in H_2 solubility and the increase in water content in the gas phase. Furthermore, higher gas partial pressure can enhance the mass transfer effect of H_2. At an absolute pressure of 9 bar, the conversion

efficiency of H_2 can reach 98.02% [61]. pH is recognized as one of the most critical and sensitive operational parameters governing acidogenic performance in the AF systems, while it also governs microbial metabolic activity [62]. Consequently, optimal operational parameters are fundamental for efficient H_2 and carboxylic acid co-production.

Bioreactor hydrodynamics critically govern interfacial gas transfer efficiency. Liquid viscosity represents a key determinant in these systems. Despite hydrogen's inherently low aqueous solubility [2], dissolved H_2 concentration supersaturation can develop in fermentation broths due to inadequate gas–liquid mass transfer [63]. When gas desorption kinetics are insufficient relative to production rates [64], dissolved H_2 concentrations exceed Henry's law equilibrium predictions, reducing proportional accumulation in the gaseous phase. Mass transfer efficiency in bioreactors is intrinsically governed by the hydrodynamic state of the fermentation broth. Laminar flow regimes impede hydrogen desorption due to suppressed interfacial turbulence, whereas heterogeneous flows enhance phase transfer through eddy-driven boundary layer renewal [63]. Crucially, reactor geometry (e.g., impeller design, baffle configuration) directly modulates broth rheology, altering viscosity profiles and gas retention dynamics in non-Newtonian systems [65]. The mass transfer coefficient demonstrates functional dependence on fundamental physicochemical properties of the reaction medium (viscosity, density, surface tension), molecular diffusivity of dissolved species, and rheological modifications induced by biochemical metabolites [59]. Agitation enhances mass transfer efficiency primarily through bubble fragmentation and phase homogenization. Impeller-generated shear forces reduce gas bubble diameter, expanding interfacial area and improving oxygen dissolution kinetics. Concurrently, sustained suspension of microbial biomass promotes uniform substrate accessibility. However, elevated agitation intensities incur significant viscous dissipation, inducing localized temperature excursions that may deviate from enzymatic optimum ranges. Such thermal gradients compromise metabolic fidelity in temperature-sensitive bioprocesses. Implementation of active cooling systems is therefore essential to maintain optimal reaction thermodynamics.

Reactor geometry fundamentally modulates hydrodynamic homogeneity, directly governing gas–liquid mass transfer kinetics in the fermentation broth. Concurrently, it dictates hydrolytic acidifying bacterial viability through shear stress distribution and substrate accessibility, critically determining bioconversion thermodynamics and acidogenesis efficiency in AF processes. These interdependencies establish reactor design as a cardinal parameter for industrial-scale H_2 and carboxylic acid co-production optimization [66]. A stirred reactor configuration enhanced hydrogen productivity by 38.7%, with yields increasing from 87.5 to 121.4 $mL \cdot g \cdot VS^{-1}$ [67]. Enhanced hydrodynamic mixing promotes bacterium–substrate interactions and facilitates hydrogen desorption from the fermentation broth. Nevertheless, contemporary H_2 and carboxylic acid co-production research predominantly employs static cultivation systems, focusing on metabolic optimization through feedstock selection/pretreatment, high-yield strain isolation, and trace metal supplementation [68]. Critical operational parameters, including hydraulic retention time distribution, dynamic flow regimes, and turbulence intensity, remain insufficiently characterized, despite their demonstrable impact on phase-transfer kinetics.

4. Regulation of Hydrogen and Carboxylic Acid Co-Production

4.1. Regulation of Hydrogen and Carboxylic Acid Concentration

H_2 and carboxylic acids partition between the fermentation broth and headspace, establishing phase equilibria governed by Henry's law. Dissolved H_2 concentration modulates cellular metabolism by inhibiting hydrogenase activity, thereby suppressing NAD^+ regeneration and redirecting carbon flux toward acidogenesis. This dissolved-phase H_2 partial pressure constitutes the primary thermodynamic driving force for gas–liquid mass

transfer. Current limitations in real-time dissolved H_2 concentration monitoring impede direct quantification of liquid-phase H_2 concentrations during fermentation [63]. Consequently, research prioritizes metabolic inhibition mitigation [41,56], including physical displacement (sparging with inert gases (N_2/CO_2) to reduce dissolved partial pressure), thermodynamic modulation (system pressure reduction to amplify desorption driving force), interfacial engineering (agitation intensification and surface area augmentation), and process innovation (recirculation of H_2-enriched biogas to dilute metabolic inhibitors) [57]. Targeted modulation of dissolved H_2 partial pressure, enables synergistic enhancement of H_2 and carboxylic acid co-production. This dissolved H_2 management paradigm constitutes a foundational research paradigm for co-production systems, enabling synergistic carbon flux partitioning between gaseous (H_2) and liquid-phase (carboxylic acids) products through targeted metabolic uncoupling. Table 2 evaluates the relative merits and limitations of key regulatory techniques.

Table 2. Comparison of regulation techniques of hydrogen concentration enhancing carboxylic acids and hydrogen co-production.

Regulation Techniques	Advantages	Disadvantages	Ref.
Gas stripping	1. Accelerating system mass transfer 2. Relieving the inhibition of hydrogen partial pressure	1. Dilution of the generated biogas 2. The difficult of separating N_2 and H_2 3. CO_2 stripping induces system acidification through carbonic acid dissociation	[49,57]
Vigorous stir	1. Accelerating system mass transfer 2. Increasing the contact area between microorganisms and substrates	1. Increasing operating costs 2. Breaking down the biological flocs	[69]

Inert gas sparging mitigates dissolved H_2 inhibition in co-production systems by reducing liquid-phase partial pressure through thermodynamic displacement. Stripping with N_2 can increase the hydrogen and carboxylic acid co-production rate by almost 70% [70]. Sekoai's study [71] demonstrated that during the anaerobic fermentation of potato waste, N_2 sparging significantly increased the yields of hydrogen and carboxylic acids by 2.5-fold and 1.8-fold, respectively. The highest proportion of biohydrogen reached was 56.98%, with a corresponding total biohydrogen production of 294.83 mL H_2/g total volatile solids. In addition, N_2 sparging can inhibit the activity of methanogens and promote the accumulation of volatile fatty acids. However, inert gas sparging incurs significant biogas dilution, reducing hydrogen partial pressure in the headspace, N_2-mediated stripping introduces additional downstream separation complexity [49]. This renders N_2 economically impractical for industrial implementation despite its metabolic efficacy. Biogas recirculation (H_2/CO_2) achieves comparable gas–liquid mass transfer enhancement of inert gas injection without diluting combustible gas content. Critically, CO_2 exhibits superior separability from H_2 via alkaline absorption, positioning this as a scalable technology [57]. However, CO_2 dissolution depresses system pH through carbonic acid formation ($H_2CO_3 \leftrightarrow H^+ + HCO_3^-$), potentially inhibiting hydrogenase activity beyond $\Delta pH > 0.5$. Strategic alkali supplementation is therefore essential to maintain optimal pH for hydrolytic acidifying bacteria [70]. While studies confirm that hydrodynamic agitation enhances multiphase mass transfer, yielding quantifiable improvements in H_2 and carboxylic acid co-production efficiency, industrial implementation faces critical scalability constraints. Vigorous impeller-driven mixing incurs prohibitive power consumption. This manifests in unsustainable operating expenditures of product value in commercial biorefineries, rendering high-shear strategies economically nonviable despite their biochemical efficacy [69]. Moreover, hydrodynamic shear regimes sufficient to mitigate dissolved H_2 supersaturation exceed the critical shear

tolerance of H_2 and carboxylic acid co-production [63]. Impeller-induced stress disrupts microbial floc integrity and induces community structure shifts [72]. This fragmentation severs syntrophic relationships, impairing reactor resilience and H_2 and carboxylic acid co-production efficiency by compromising interspecies electron transfer kinetics [73].

Hydrogen and organic carboxylic acid production is interdependent. An increase in hydrogen partial pressure suppresses acid-forming bacteria, reducing organic carboxylic acid production [74]. Conversely, organic carboxylic acids produced during fermentation inhibit microbial metabolic activities, thus diminishing hydrogen production. To decrease undissociated carboxylic acids levels, the fermentation broth's pH can be raised to enhance carboxylic acid dissociation. Alkaline or buffer solutions are commonly used for pH stabilization [75]. Nevertheless, alkaline solutions may cause inorganic salt accumulation, harming microbial activity [76]. In situ carboxylic acid removal from the fermentation broth is considered optimal. Current effective methods for organic carboxylic acid recovery from anaerobic fermentation broth include liquid–liquid extraction, ion exchange, pervaporation, and membrane separation [77], but they all have drawbacks, such as high solvent requirements, regeneration needs, or back-extraction complexities.

While existing dissolved H_2 mitigation strategies partially alleviate metabolic inhibition, their inherent limitations necessitate fundamentally distinct approaches. The equilibrium concentrations of both dissolved H_2 and undissociated carboxylic acids constitute primary thermodynamic constraints on co-production kinetics. Implementing targeted product extraction via continuous phase-separation driving forces represents the only pathway to transcend these concentration barriers while avoiding secondary operational compromises.

4.2. Bioreactor Configuration Optimization

Reactor topology fundamentally dictates H_2 and carboxylic acid ecosystem functionality by governing spatial distribution of microbial consortia, interfacial mass transfer kinetics, and thermodynamic boundary conditions. Precision control of process parameters, particularly hydraulic retention time (HRT), organic loading rate (OLR), and phase-separation efficiency, enables metabolic steering toward synergistic H_2 and carboxylic acid co-production [78]. Figure 5 comparatively evaluates the relative merits and limitations of different reactor configurations in H_2 and carboxylic acid co-production.

The continuously stirred tank reactor (CSTR) remains the predominant configuration for continuous H_2 and carboxylic acid co-production due to operational robustness and process intensification capabilities. Its axiomatic design facilitates perfect mixing kinetics, elimination of substrate gradients, and a sustained homogenized reaction environment for uniform biomass–substrate contact [79]. Agitation simultaneously enhances hydrogen stripping from fermentation broth, inducing system depressurization that elevates co-production rates of hydrogen and carboxylic acids. However, biomass concentration remains constrained by HRT, a critical determinant of hydrogenogenic activity [29]. Critically, bacterial activity diminishes at low biomass concentrations, necessitating HRT shorter than the microbial growth cycle to optimize H_2 and carboxylic acid co-production [79]. Consequently, microbial immobilization techniques, both biological and physical, have been implemented to enhance biomass retention, significantly improving CSTR productivity. In Oshiki et al.'s study, when breadcrumbs were used as the raw material in a 3 L CSTR and operated for 269 days, the production of acetate and butyrate on day 52 achieved the highest H_2 production rate of 7.0 L H_2/(L·d) [80]. Furthermore, impeller geometry and agitation rate critically modulate H_2–carboxylate co-production in CSTR systems. Optimized impeller design ensures efficient mixing and mass transfer while minimizing biomass shear

stress. Gabriel et al. [81] quantified this relationship, demonstrating that rotational speed significantly governs co-production yields during continuous operation.

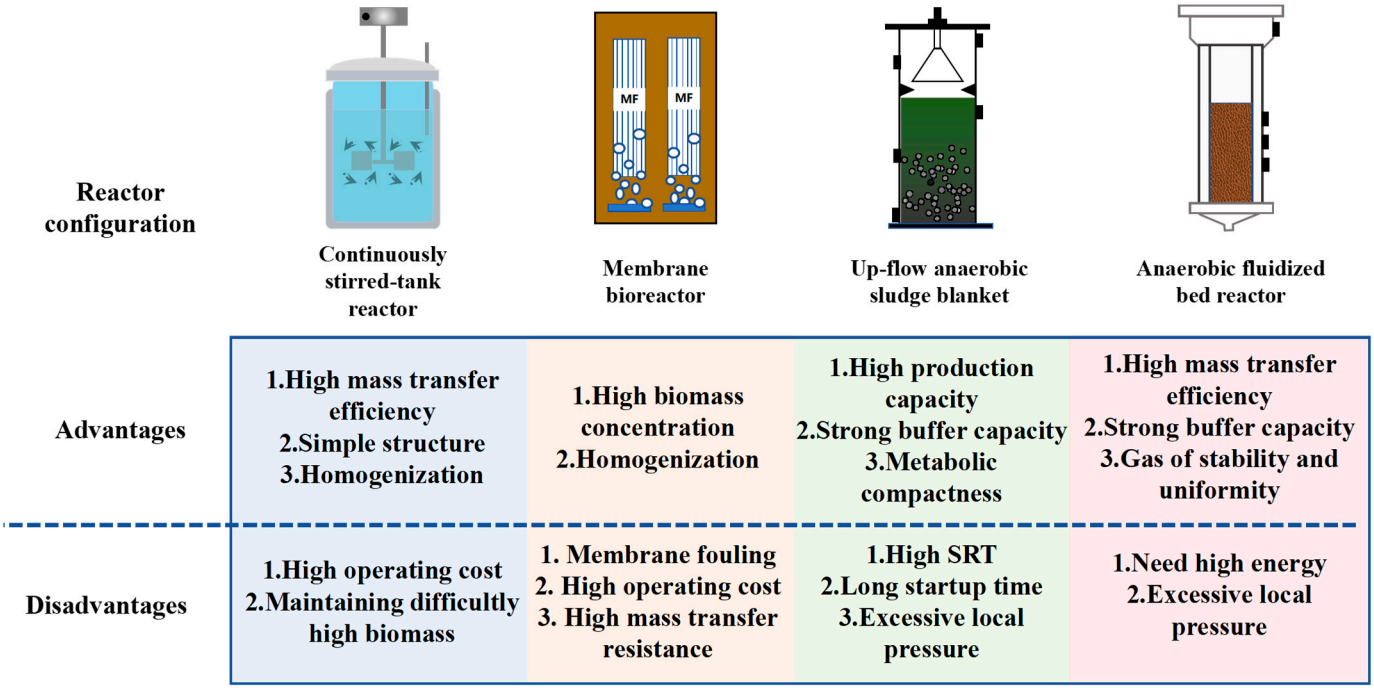


Figure 5. Compared reactor configuration enhancing carboxylic acid and hydrogen co-production.

The membrane bioreactor (MBR) integrates activated sludge treatment with membrane filtration, effectively retaining microbial biomass and eliminating washout limitations inherent to CSTR systems [29]. This retention capability enables elevated solid retention times (SRT), enhancing substrate conversion efficiency and volumetric productivity [82]. Solute transport across membranes is driven by transmembrane chemical potential gradients, operating through diffusion and/or convection mechanisms. This process inherently couples mass transfer dynamics with hydrodynamic conditions [83]. Recent advances in membrane bioreactor technology include liquid–gas systems designed to optimize anaerobic fermentation. Hollow-fiber configurations consolidate multiple functions retention of H_2 and carboxylic acid co-production, in situ gas–liquid separation, and confinement of acidogenic microorganisms within a unified reactor environment. Marie et al. [84] achieved peak hydrogen productivity (1.22 mol H_2/mol glucose) at 13.1 g/L glucose loading using liquid–gas membrane bioreactor technology. This configuration facilitated two-phase (gas–liquid) cross-flow, where elevated liquid velocities in bubble-induced falling films and vortex generation during bubble ascent enhanced mass transfer kinetics through boundary layer disruption [85]. This enabled membrane module engineering for uniform, high-intensity scouring in two-phase flow systems, effectively mitigating scaling. However, Zhang et al. [86] demonstrated that bubble size and formation frequency critically modulate hydrodynamic behavior through boundary layer disruption efficiency, shear stress distribution, and local turbulence intensity. Electrodialysis (ED) represents an emerging membrane technology that enhances AF by continuously extracting carboxylic acids, thereby boosting H_2 and carboxylic acid co-production [87]. Nevertheless, membrane fouling and elevated operational expenditures constrain its industrial implementation.

Packed-bed bioreactors (PBRs) typically retain microorganisms in three configurations: suspended particles, surface-adhered biofilms, or gel-immobilized biomass [88]. Among high-rate anaerobic systems, upflow anaerobic sludge blanket (UASB) reactors represent the most prevalent configuration for biomass retention. UASB reactors exhibit superior H_2

and carboxylic acid co-production capacity due to their self-granulating microbial consortia, which demonstrate enhanced substrate degradation kinetics [89]. The granular structure enables high biomass retention and confers heightened tolerance to inhibitory conditions. This metabolic compactness further optimizes substrate conversion thermodynamics toward co-production pathways. Notably, Afridi et al. [90] found a direct correlation between granular particle size and mass transfer kinetics in UASB reactors. Mass transfer efficiency exhibited vertical heterogeneity, with the bottom zone demonstrating superior kinetics to middle and upper regions. Furthermore, buoyancy-driven bubble ascent during fermentation generated convective turbulence, enhancing medium mixing through vortical dissipation [91]. However, UASB systems face significant constraints, biomass washout in effluent, prolonged start-up periods, and excessively high SRT. Notably, mass transfer rates exhibit positive correlations with OLR. Both convective and molecular transfer mechanisms operate within UASBs, though their efficiency decreases inversely with reactor height. Enhanced biogas recovery efficiency stems from accelerated mass transfer kinetics in lower zones [92]. To mitigate limitations, researchers have integrated microbial carriers to augment biomass retention and boost H_2 and carboxylic acid productivity.

Anaerobic fluidized bed reactors (AFBRs) integrate the continuous mixing of CSTRs with the attached-growth design of fixed-bed systems. Microorganisms immobilize as biofilms on granular media or carrier surfaces [91]. Compared with CSTR, AFBRs demonstrate superior fluidization-driven mixing, reduced hydrodynamic shear, and enhanced mass transfer efficiency. Biomass retention exceeds conventional reactors due to microbial attachment, significantly reducing washout risks. This immobilized configuration concurrently elevates substrate conversion rates relative to suspended-growth systems. Crucially, the selection of support material governs AFBR performance efficiency. During reactor operation, biofilm formation on these substrates enables high-density biomass retention [93]. Documented support matrices for H_2 and carboxylic acid co-production include activated carbon, diatomaceous earth, and expanded clay. Encina et al. [94] demonstrated that heterogeneous biofilm accretion induces particle size–density stratification, disrupting fluidized bed hydrodynamics. This spatial heterogeneity reduced fluidization homogeneity, elevated local mass transfer resistance, and created dead zones. Table 3 compares the yields of hydrogen and carboxylic acids in different bioreactors.

Table 3. Yields of hydrogen and carboxylic acids in different bioreactors.

Reactor Type	Substrate	H_2 Production Rate	Yield of Carboxylic acid	Ref.
CSTR	Waste pastry hydrolysate	The maximum hydrogen production rate (HPR) of CSTR (277.76 mL/(h·L) was achieved at OLR of 24 kgCOD/(m^3·d)	Acetic acid (HAc) serves as the primary product, reaching a concentration of up to 13.85 mmol/L.	[95]
CSTR	Fruit-vegetable waste	When HRT is 6 h, the highest HPR can reach 11.8 NL·L-d^{-1}.	Lactic acid is the main product, and its concentration can reach up to 18.4 ± 1.2 g/L.	[96]
CSTR	Breadcrumbs	The highest HPR was 7.0 L-H_2·L^{-1}·d^{-1}	181 mM of HAc	[80]
MBR	Medium	The average HPR was 106.5 ± 10.6 mL-H_2·L-medium^{-1}·h^{-1}	HAc and butyric acid (HBc), the main products, can be produced at rates of 0.8–1.6 mmol/L/h and 1.1–2.2 mmol/L/h, respectively.	[84]
MBR	Synthetic feed containing sucrose	The highest HPR was 0.95 L-H_2 L^{-1}·d^{-1}	HAc and HBc are the main products, with the highest concentrations reaching 79 mM and 96 mM, respectively.	[97]

Table 3. *Cont.*

Reactor Type	Substrate	H_2 Production Rate	Yield of Carboxylic acid	Ref.
UASB	Galactose	When the hydraulic retention time is 2 h, the maximum HPR can reach 56.8 $L \cdot L^{-1} \cdot d^{-1}$.	HAc and HBc, as the main soluble metabolites, can reach concentrations of up to 1700–2100 mg/L and 3500–3950 mg/L, respectively.	[98]
UASB	Palm oil mill effluent	The maximum HPR can achieved 11.75 $L \cdot L^{-1} \cdot d^{-1}$	HAc is the main soluble product, with a maximum concentration of 550 mM.	[99]
AFBR	vinasse and cheese whey	2.54 ± 0.39 L $H_2 \cdot d^{-1} \cdot L^{-1}$	HAc and HBc are the main soluble products, with maximum percentages reaching 29.5% and 23.3%, respectively.	[100]

4.3. Coupling with Microbial Electrolysis Cell

The microbial electrolysis cell (MEC) is a bioelectrochemical technology employing electrogenic microorganisms to co-produce H_2 and carboxylic acids from organic substrates [101]. Common MEC configurations include single-chamber and two-chamber reactors. Within these systems, organic matter is oxidized by electrogenic bacteria on the anode, generating CO_2, protons (H^+), and electrons. The bacteria transfer electrons to the anode while releasing protons into the solution. These electrons then travel via an external circuit (under applied potential) to the cathode, where they combine with free protons to form H_2 and carboxylic acids [102]. Figure 6 illustrates the integration of MEC with AF to enhance co-production of these target compounds.

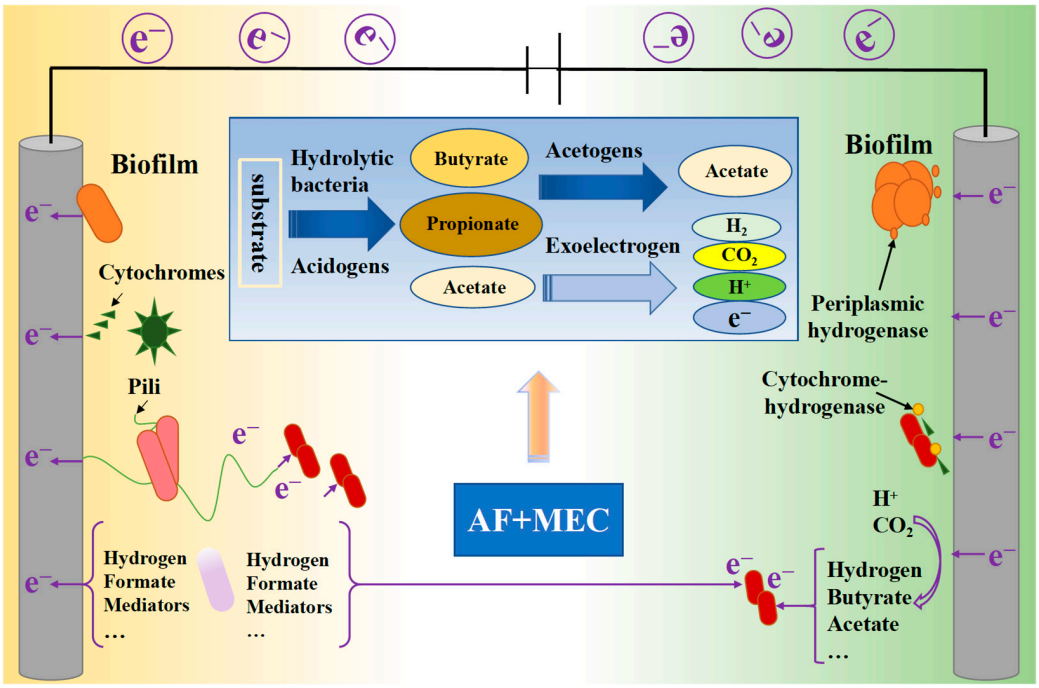


Figure 6. Anaerobic fermentation coupled with microbial electrolytic cell for carboxylic acids and hydrogen co-production.

While MECs exhibit constraints as standalone systems for hydrogen and carboxylic acid co-production, primarily due to the inability of anode-respiring bacteria to metabolize complex organic wastewater and waste streams [103], they demonstrate high efficiency when processing defined substrates. These systems achieve yields of 70%–90% for target

products using pure cultures, co-cultures, or mixed consortia with fermentable compounds like glucose and cellulose [104]. Consequently, the synergistic integration of MEC with AF unlocks significant operational advantages by combining substrate versatility with electrochemical efficiency. MECs enable secondary valorization of AF effluent, biochemically converting residual organics into additional H_2 and carboxylic acids. Chookaew et al. [105] evaluated AF effluent utilization as an MEC substrate, demonstrating enhanced hydrogen yield and COD (chemical oxygen demand) removal under electrochemical treatment. At 1.0 V applied potential, the system achieved 106 mL H_2/g-COD hydrogen production, doubling COD removal efficiency from 20% (AF alone) to 41%. Collectively, these findings validate the integrated AF–MEC process as a highly efficient pathway for enhancing H_2 and carboxylic acid co-production, leveraging synergistic substrate conversion.

The CO_2 produced by MEC anodes is emitted directly into the atmosphere, which not only results in a waste of carbon resources but also reduces the overall environmental benefits of the system [106]. In recent years, the integration of carbon capture technology into MECs has provided an innovative solution to the problem of CO_2 emissions from anode reactions while opening new avenues for enhanced hydrogen and carboxylic acid production [107]. CO_2 can significantly enhance H_2 production by modulating the MEC microenvironment, optimizing microbial metabolism and electron transfer efficiency. Through the formation of an H_2CO_3–HCO_3^- buffer pair (pKa $\approx$ 6.4), the captured CO_2 can stabilize the pH of the reaction system at 6.0–7.0. This will help to maintain the metabolic activity of the electroactive microorganisms and prevent the overly acidic environment from destroying their cell membranes and enzyme activities, which will increase the anode's electron generation efficiency [108]. In addition, MEC can utilize electroactive bacteria and homoacetogens to mediate the reduction of CO_2 to volatile fatty acids [109] such as acetic [110], butyric [111], and caproic [106]. The integration of carbon capture with MEC enables high-value conversion of CO_2 and provides a sustainable technology pathway for hydrogen and carboxylic acid co-production under the "dual carbon" goal.

5. Conclusions

The co-production of carboxylic acids and hydrogen has been established as a fossil energy alternative with dual value as both energy carriers and chemical feedstocks. Within existing technological frameworks, anaerobic fermentation-based pathways for carboxylic acids and hydrogen co-production demonstrate significant potential. The co-production of carboxylic acids and hydrogen demonstrates strong economic viability due to the numerous benefits of low-cost feedstock use, energy efficiency optimization, and high-value product integration. The economics of anaerobic fermentation center on feedstock cost control. Current processes have efficiently converted low-cost feedstocks such as agricultural waste, industrial wastewater, and municipal organic waste into target products. Life-cycle assessments show that anaerobic fermentation systems have a carbon footprint that is 60%–80% lower than conventional fossil fuel routes. Furthermore, fermentative VFA production demonstrated 1.7-fold, 2.6-fold, and 6.8-fold reductions in environmental impact scores for human health, climate change, and resource consumption, respectively, compared to conventional fossil-based processes [112]. With the synergistic effect of cost savings and emission reduction benefits, the technology route of anaerobic fermentation for the co-production of hydrogen and carboxylic acids offers an industrial-scale solution with great potential and environmental sustainability for organic waste resource utilization.

However, current yields and purity profiles of carboxylic acids and hydrogen in AF systems remain suboptimal. Inefficient gas–liquid mass transfer constitutes a core limitation in these systems, where multiphase transport processes are governed by multivariate coupling effects within complex fermentation microenvironments. Although interventions

such as gas stripping and mechanical agitation can enhance carboxylic acid enrichment and hydrogen production, they incur substantial energy penalties and risk triggering metabolic inhibition. Integrating anaerobic acidogenic fermentation with other technologies such as microbial electrolysis cells offers a promising paradigm, thereby establishing more robust co-production systems. In the future, the development of low-cost electrode materials will accelerate the large-scale application of MECs, enhancing the hydrogen production rate while reducing costs by 70% to 90%. The design of synthetic microbial communities will become the key to enhancing the efficiency of co-production. By optimizing the metabolic pathways of acid-producing bacteria and hydrogen-producing bacteria through gene editing technology, substrate transformation efficiency can be specifically enhanced. In addition, real-time control systems driven by intelligence and digitalization will become the core tools for process optimization. Dynamic optimization of parameters is achieved by integrating multi-dimensional data such as temperature, pH, and stirring speed. The efficient co-production of hydrogen and carboxylic acids through anaerobic fermentation may offer a solution with dual environmental and economic benefits for technological innovations in organic waste treatment in the context of global carbon neutrality.

Author Contributions: X.X.: conceptualization, literature survey, writing—original draft. M.H., Y.H.: writing—review and editing, investigation. B.A.S.: writing—review and editing. W.D., C.L.: writing—review and editing, validation, supervision, conceptualization. B.Y.: writing—review and editing, conceptualization and visualization. All authors have read and agreed to the published version of the manuscript.

Funding: This research received no external funding.

Acknowledgments: The authors express heartfelt gratitude to Yan and Luo from the School of Environment and Ecology at Hunan Agricultural University for their invaluable guidance and support over the years, as well as to the research team for their assistance.

Conflicts of Interest: The authors declare that they have no known competing financial interests or personal relationships that could have appeared to influence the work reported in this paper.

Abbreviations

The following abbreviations and symbols are used in this manuscript:

AF	Anaerobic fermentation
NAD^+	Adenine dinucleotide ion
NADH	Nicotinamide adenine dinucleotide
Acetyl-CoA	Acetyl coenzyme A
PFL	Pyruvate formate lyase
PFOR	Pyruvate-ferredoxin oxidoreductase
FNOR	Ferredoxin-dependent $NADP^+$ oxidoreductase
FHL	Formate hydrogen lyase
AET	Acetate–ethanol-type fermentation
BTF	Butyrate fermentation
PPF	Propionate fermentation
PTB	Phosphotransbutyrylase
BK	Butyrate kinase
APB	Acid-producing bacteria
HRT	Hydraulic retention time
SRT	Solid retention time
OLR	Organic loading rate
CSTR	Continuously stirred tank reactor
MBR	Membrane bioreactor
UASB	Upflow anaerobic sludge blanket

AFBR	Anaerobic fluidized bed reactor
PBR	Packed-bed bioreactor
MEC	Microbial electrolysis cell
COD	Chemical oxygen demand
K_H^i	Henry's constant for gas *i* ($m^3 \cdot Pa \cdot mol^{-1}$)
P_G^i	Partial pressure of gas *i* in the gas phase (Pa)
C_F^i	Dissolved concentration of gas *i* in the liquid phase ($mol \cdot m^{-3}$)
N_A	Mass transfer flux ($mol \cdot s^{-1} \cdot m^2$)
k	Mass transfer coefficient ($m \cdot s^{-1}$)
$C_{Ai} - C_A$	Concentration difference between the two phases ($mol \cdot m^3$)
C_0	Initial concentration of substances ($mol \cdot m^{-3}$);
C_{av}	Concentration of substances at the gas–liquid interface ($mol \cdot m^{-3}$)
C_e	Equilibrium concentration of substances in the gas–liquid phase ($mol \cdot m^{-3}$)
E_f	Mass transfer efficiency
t	Mass transfer time (s)
K_L	Liquid-side mass transfer coefficient ($m \cdot s^{-1}$)
a	Interface area ($m^2 \cdot m^{-3}$)
Q	Molar gas transfer rate ($mol \cdot s^{-1}$)
K_La	Volumetric mass transfer coefficient (s^{-1})
P_G	Partial pressure in the gas phase (Pa)
P_G°	Equilibrium partial pressure (Pa)
H	Henry's constant ($Pa \cdot m^3 \cdot mol^{-1}$)

References

1. Posso, F.; Galeano, M.; Baranda, C.; Franco, D.; Rincón, A.; Zambrano, J.; Cavaliero, C.; Lópes, D. Towards the hydrogen economy in paraguay: Green hydrogen production potential and end-uses. *Int. J. Hydrogen Energy* **2022**, *47*, 30027–30049. [CrossRef]
2. Nemestóthy, N.; Bélafi-Bakó, K.; Bakonyi, P. Enhancement of dark fermentative H_2 production by gas separation membranes: A review. *Bioresour. Technol.* **2020**, *302*, 122828. [CrossRef] [PubMed]
3. Rai, P.; Gupta, P.; Saini, N.; Tiwari, A.K. Assessing the impact of renewable energy and non-renewable energy use on carbon emissions: Evidence from select developing and developed countries. *Environ. Dev. Sustain.* **2025**, *27*, 3059–3080. [CrossRef]
4. Wang, Z.; Li, S.; Jin, Z.; Li, Z.; Liu, Q.; Zhang, K. Oil and gas pathway to net-zero: Review and outlook. *Energy Strateg. Rev.* **2023**, *45*, 101048. [CrossRef]
5. Zhou, X.; Xie, F.; Li, H.; Zheng, C.; Zhao, X. Understanding inter-term fossil energy consumption pathways in China based on sustainable development goals. *Geosci. Front.* **2024**, *15*, 101687. [CrossRef]
6. Fayyazbakhsh, A.; Bell, M.L.; Zhu, X.; Mei, X.; Koutný, M.; Hajinajaf, N.; Zhang, Y. Engine emissions with air pollutants and greenhouse gases and their control technologies. *J. Clean. Prod.* **2022**, *376*, 134260. [CrossRef]
7. Liu, G.; Li, M.; Zhou, B.; Chen, Y.; Liao, S. General indicator for techno-economic assessment of renewable energy resources. *Energy Convers. Manag.* **2018**, *156*, 416–426. [CrossRef]
8. Bhatt, A.H.; Ren, Z.J.; Tao, L. Value proposition of untapped wet wastes: Carboxylic acid production through anaerobic digestion. *iScience* **2020**, *23*, 101221. [CrossRef] [PubMed]
9. Olokede, O.; Wu, H.; Holtzapple, M. Valorizing prickly pear cladodes via methane-arrested anaerobic digestion for carboxylic acid production. *Biotechnol. Prog.* **2022**, *38*, e3289. [CrossRef] [PubMed]
10. Arimi, M.M.; Knodel, J.; Kiprop, A.; Namango, S.S.; Zhang, Y.; Geißen, S. Strategies for improvement of biohydrogen production from organic-rich wastewater: A review. *Biomass Bioenerg.* **2015**, *75*, 101–118. [CrossRef]
11. Qian, Q.; Zhang, J.; Cui, M.; Han, B. Synthesis of acetic acid via methanol hydrocarboxylation with CO_2 and H_2. *Nat. Commun.* **2016**, *7*, 11481. [CrossRef] [PubMed]
12. Kelbert, M.; Machado, T.O.; Araújo, P.H.H.; Sayer, C.; de Oliveira, D.; Maziero, P.; Simons, K.E.; Carciofi, B.A.M. Perspectives on biotechnological production of butyric acid from lignocellulosic biomass. *Renew. Sustain. Energy Rev.* **2024**, *202*, 114717. [CrossRef]
13. Wang, Y.; Li, G.; Liu, Z.; Cui, P.; Zhu, Z.; Yang, S. Techno-economic analysis of biomass-to-hydrogen process in comparison with coal-to-hydrogen process. *Energy* **2019**, *185*, 1063–1075. [CrossRef]
14. Boretti, A.; Banik, B.K. Advances in Hydrogen Production from Natural Gas Reforming. *Adv. Energy Sustain. Res.* **2021**, *2*, 2100097. [CrossRef]

15. Shi, X.; Wu, L.; Wei, W.; Ni, B. Insights into the microbiomes for medium-chain carboxylic acids production from biowastes through chain elongation. *Crit. Rev. Environ. Sci. Technol.* **2022**, *52*, 3787–3812. [CrossRef]
16. Das, D.; Veziroğlu, T.N. Hydrogen production by biological processes: A survey of literature. *Int. J. Hydrogen Energy* **2001**, *26*, 13–28. [CrossRef]
17. Chen, Y.; Yin, Y.; Wang, J. Influence of butyrate on fermentative hydrogen production and microbial community analysis. *Int. J. Hydrogen Energy* **2021**, *46*, 26825–26833. [CrossRef]
18. Zhou, M.; Yan, B.; Wong, J.W.C.; Zhang, Y. Enhanced volatile fatty acids production from anaerobic fermentation of food waste: A mini-review focusing on acidogenic metabolic pathways. *Bioresour. Technol.* **2018**, *248*, 68–78. [CrossRef] [PubMed]
19. Qu, X.; Zeng, H.; Gao, Y.; Mo, T.; Li, Y. Bio-hydrogen production by dark anaerobic fermentation of organic wastewater. *Front. Chem.* **2022**, *10*, 978907. [CrossRef] [PubMed]
20. Yang, Y.; Liu, C.; Zhao, W.; Mazarji, M.; Ren, L.; Liu, C.; Pan, J.; Yan, B. Anaerobic propionic acid production via succinate pathway at extremely low pH. *Chem. Eng. J.* **2024**, *486*, 150190. [CrossRef]
21. Horiuchi, J.I.; Shimizu, T.; Tada, K.; Kanno, T.; Kobayashi, M. Selective production of organic acids in anaerobic acid reactor by pH control. *Bioresour. Technol.* **2002**, *82*, 209–213. [CrossRef] [PubMed]
22. Li, Y.; Huang, W.; Fang, S.; Li, Z.; Li, Z.; Wang, F.; Cheng, X.; Cao, J.; Feng, L.; Luo, J.; et al. Zinc pyrithione induced volatile fatty acids promotion derived from sludge anaerobic digestion: Interrelating the affected steps with microbial metabolic regulation and adaptive responses. *Water Res.* **2023**, *234*, 119816. [CrossRef] [PubMed]
23. Dahiya, S.; Lingam, Y.; Venkata Mohan, S. Understanding acidogenesis towards green hydrogen and volatile fatty acid production—Critical analysis and circular economy perspective. *Chem. Eng. J.* **2023**, *464*, 141550. [CrossRef]
24. Ceron-Chafla, P.; Kleerebezem, R.; Rabaey, K.; van Lier, J.B.; Lindeboom, R.E.F. Direct and indirect effects of increased CO_2 partial pressure on the bioenergetics of syntrophic propionate and butyrate conversion. *Environ. Sci. Technol.* **2020**, *54*, 12583–12592. [CrossRef] [PubMed]
25. Abdelgadir, A.; Chen, X.; Liu, J.; Xie, X.; Zhang, J.; Zhang, K.; Wang, H.; Liu, N.; Tang, C. Characteristics, process parameters, and inner components of anaerobic bioreactors. *BioMed Res. Int.* **2014**, *2014*, 841573. [CrossRef] [PubMed]
26. Lovley, D.R.; Nevin, K.P. Electrobiocommodities: Powering microbial production of fuels and commodity chemicals from carbon dioxide with electricity. *Curr. Opin. Biotechnol.* **2013**, *24*, 385–390. [CrossRef] [PubMed]
27. Strazzera, G.; Battista, F.; Garcia, N.H.; Frison, N.; Bolzonella, D. Volatile fatty acids production from food wastes for biorefinery platforms: A review. *J. Environ. Manag.* **2018**, *226*, 278–288. [CrossRef] [PubMed]
28. Yang, G.; Wang, J. Various additives for improving dark fermentative hydrogen production: A review. *Renew. Sustain. Energy Rev.* **2018**, *95*, 130–146. [CrossRef]
29. Li, C.; Fang, H.H.P. Fermentative hydrogen production from wastewater and solid wastes by mixed cultures. *Crit. Rev. Environ. Sci. Technol.* **2007**, *37*, 1–39. [CrossRef]
30. Voldsund, M.; Jordal, K.; Anantharaman, R. Hydrogen production with CO_2 capture. *Int. J. Hydrogen Energy* **2016**, *41*, 4969–4992. [CrossRef]
31. Lee, H.; Salerno, M.B.; Rittmann, B.E. Thermodynamic Evaluation on H_2 Production in Glucose Fermentation. *Environ. Sci. Technol.* **2008**, *42*, 2401–2407. [CrossRef] [PubMed]
32. Taheri, E.; Amin, M.; Pourzamani, H.; Fatehizadeh, A.; Ghasemian, M.; Bina, B. Comparison of acetate-butyrate and acetate-ethanol metabolic pathway in biohydrogen production. *J. Med. Signals Sens.* **2018**, *8*, 101–107. [CrossRef] [PubMed]
33. Saady, N.M.C. Homoacetogenesis during hydrogen production by mixed cultures dark fermentation: Unresolved challenge. *Int. J. Hydrogen Energy* **2013**, *38*, 13172–13191. [CrossRef]
34. Rahimieh, A.; Nosrati, M. A review on biochemistry, microbiology and thermodynamic aspects of propionate: The key intermediate in the anaerobic digestion and wastewater treatment. *Desalin Water Treat.* **2024**, *317*, 100191. [CrossRef]
35. Zhang, S.; Liu, M.; Chen, Y.; Pan, Y. Achieving ethanol-type fermentation for hydrogen production in a granular sludge system by aeration. *Bioresour. Technol.* **2017**, *224*, 349–357. [CrossRef] [PubMed]
36. Chong, M.; Sabaratnam, V.; Shirai, Y.; Hassan, M.A. Biohydrogen production from biomass and industrial wastes by dark fermentation. *Int. J. Hydrogen Energy* **2009**, *34*, 3277–3287. [CrossRef]
37. Ciranna, A.; Ferrari, R.; Santala, V.; Karp, M. Inhibitory effects of substrate and soluble end products on biohydrogen production of the alkalithermophile Caloramator celer: Kinetic, metabolic and transcription analyses. *Int. J. Hydrogen Energy* **2014**, *39*, 6391–6401. [CrossRef]
38. Khanal, S.K.; Chen, W.; Li, L.; Sung, S. Biological hydrogen production: Effects of pH and intermediate products. *Int. J. Hydrogen Energy* **2004**, *29*, 1123–1131. [CrossRef]
39. Grupe, H.; Gottschalk, G. Physiological Events in Clostridium acetobutylicum during the Shift from Acidogenesis to Solventogenesis in Continuous Culture and Presentation of a Model for Shift Induction. *Appl. Environ. Microb.* **1992**, *58*, 3896–3902. [CrossRef] [PubMed]

40. Beckers, L.; Masset, J.; Hamilton, C.; Delvigne, F.; Toye, D.; Crine, M.; Thonart, P.; Hiligsmann, S. Investigation of the links between mass transfer conditions, dissolved hydrogen concentration and biohydrogen production by the pure strain *Clostridium butyricum* CWBI1009. *Biochem. Eng. J.* **2015**, *98*, 18–28. [CrossRef]
41. Sivagurunathan, P.; Kumar, G.; Bakonyi, P.; Kim, S.; Kobayashi, T.; Xu, K.Q.; Lakner, G.; Tóth, G.; Nemestóthy, N.; Bélafi-Bakó, K. A critical review on issues and overcoming strategies for the enhancement of dark fermentative hydrogen production in continuous systems. *Int. J. Hydrogen Energy* **2016**, *41*, 3820–3836. [CrossRef]
42. Noblecourt, A.; Christophe, G.; Larroche, C.; Santa-Catalina, G.; Trably, E.; Fontanille, P. High hydrogen production rate in a submerged membrane anaerobic bioreactor. *Int. J. Hydrogen Energy* **2017**, *42*, 24656–24666. [CrossRef]
43. Tang, Z.; Zhang, J.; Yuan, X.; Wang, D.; Luo, H.; Yang, R.; Wang, H. Urea promotes alkaline anaerobic fermentation of waste activated sludge for hydrogen production. *Bioresour. Technol.* **2025**, *418*, 131900. [CrossRef] [PubMed]
44. Cui, P.; Wang, D.; Wang, S.; Su, H.; Wang, Y. Regulatory mechanism of antioxidant enzymes on microbial metabolism and NADH in anaerobic fermentation of food waste for hydrogen production. *J. Clean. Prod.* **2024**, *474*, 143607. [CrossRef]
45. Wang, X.; Ming, X.; Han, X.; Liu, Y.; Chen, M.; Zhang, T.; Li, X.; Zhang, D. Effect of lactic acid on short-chain fatty acids and hydrogen production during anaerobic fermentation of acidified food waste. *Fuel* **2025**, *386*, 134275. [CrossRef]
46. Greses, S.; Tomás-Pejó, E.; González-Fernández, C. Short-chain fatty acids and hydrogen production in one single anaerobic fermentation stage using carbohydrate-rich food waste. *J. Clean. Prod.* **2021**, *284*, 124727. [CrossRef]
47. Shi, Z.; Zhang, L.; Yuan, H.; Li, X.; Chang, Y.; Zuo, X. Oyster shells improve anaerobic dark fermentation performances of food waste: Hydrogen production, acidification performances, and microbial community characteristics. *Bioresour. Technol.* **2021**, *335*, 125268. [CrossRef] [PubMed]
48. Liu, Q.; Ji, X.; Zhu, K.; Wang, W.; Bao, Z.; Zhang, L. Biorefinery-oriented pyrolysis and anaerobic fermentation synergies: Leveraging biomass tar for enhanced chemical production from food waste. *J. Clean. Prod.* **2024**, *477*, 143830. [CrossRef]
49. Sonnleitner, A.; Peintner, C.; Wukovits, W.; Friedl, A.; Schnitzhofer, W. Process investigations of extreme thermophilic fermentations for hydrogen production: Effect of bubble induction and reduced pressure. *Bioresour. Technol.* **2012**, *118*, 170–176. [CrossRef] [PubMed]
50. Levin, D.B.; Pitt, L.; Love, M. Biohydrogen production: Prospects and limitations to practical application. *Int. J. Hydrogen Energy* **2004**, *29*, 173–185. [CrossRef]
51. Valdez-Vazquez, I.; Ríos-Leal, E.; Carmona-Martínez, A.; Muñoz-Páez, K.M.; Poggi-Varaldo, H.M. Improvement of Biohydrogen Production from Solid Wastes by Intermittent Venting and Gas Flushing of Batch Reactors Headspace. *Environ. Sci. Technol.* **2006**, *40*, 3409–3415. [CrossRef] [PubMed]
52. Ma, H.; Liu, Y.; Li, Z. The synergistic hydrogen production of bicellular fermentation systems and fluid dynamics simulation in reactor under stirring. *Bioresour. Technol. Rep.* **2023**, *22*, 101473. [CrossRef]
53. Oh, S.; Zuo, Y.; Zhang, H.; Guiltinan, M.J.; Logan, B.E.; Regan, J.M. Hydrogen production by Clostridium acetobutylicum ATCC 824 and megaplasmid-deficient mutant M5 evaluated using a large headspace volume technique. *Int. J. Hydrogen Energy* **2009**, *34*, 9347–9353. [CrossRef]
54. Laurent, B.; Serge, H.; Julien, M.; Christopher, H.; Philippe, T. Effects of hydrogen partial pressure on fermentative biohydrogen production by a chemotropic *Clostridium* bacterium in a new horizontal rotating cylinder reactor. *Energy Procedia* **2012**, *29*, 34–41. [CrossRef]
55. Castro-Carranza, A.; Vega-Hernández, P.; Nolasco, J.C.; Ladstätter-Weißenmayer, A.; Eickhoff, M.; Gutowski, J. Detection of Hydrogen Dissolved in Liquid Media: A Review and Outlook. *Phys. Status Solidi A* **2022**, *219*, 2100669. [CrossRef]
56. Bundhoo, M.A.Z.; Mohee, R. Inhibition of dark fermentative bio-hydrogen production: A review. *Int. J. Hydrogen Energy* **2016**, *41*, 6713–6733. [CrossRef]
57. Bakonyi, P.; Buitrón, G.; Valdez-Vazquez, I.; Nemestóthy, N.; Bélafi-Bakó, K. A novel gas separation integrated membrane bioreactor to evaluate the impact of self-generated biogas recycling on continuous hydrogen fermentation. *Appl. Energy* **2017**, *190*, 813–823. [CrossRef]
58. Hawkes, F.R.; Dinsdale, R.; Hawkes, D.L.; Hussy, I. Sustainable fermentative hydrogen production: Challenges for process optimisation. *Int. J. Hydrogen Energy* **2002**, *27*, 1339–1347. [CrossRef]
59. Zhang, Z.; Zhou, X.; Hu, J.; Zhang, T.; Zhu, S.; Zhang, Q. Photo-bioreactor structure and light-heat-mass transfer properties in photo-fermentative bio-hydrogen production system: A mini review. *Int. J. Hydrogen Energy* **2017**, *42*, 12143–12152. [CrossRef]
60. Sieborg, M.U.; Engelbrecht, N.; Singh, A.; Schnürer, A.; Ottosen, L.D.M.; Kofoed, M.V.W.; Sveriges, L. Unraveling the effects of temperature on mass transfer and microbiology in thermophilic and extreme thermophilic trickle bed biomethanation reactors. *Chem. Eng. J.* **2025**, *509*, 161179. [CrossRef]
61. Ullrich, T.; Lindner, J.; Bär, K.; Mörs, F.; Graf, F.; Lemmer, A. Influence of operating pressure on the biological hydrogen methanation in trickle-bed reactors. *Bioresour. Technol.* **2018**, *247*, 7–13. [CrossRef] [PubMed]
62. Ginkel, S.V.; Sung, S.; Lay, J. Biohydrogen Production as a Function of pH and Substrate Concentration. *Environ. Sci. Technol.* **2001**, *35*, 4726–4730. [CrossRef] [PubMed]

63. Zhang, F.; Zhang, Y.; Chen, M.; Zeng, R.J. Hydrogen supersaturation in thermophilic mixed culture fermentation. *Int. J. Hydrogen Energy* **2012**, *37*, 17809–17816. [CrossRef]
64. Maluta, F.; Paglianti, A.; Montante, G. Modelling of biohydrogen production in stirred fermenters by Computational Fluid Dynamics. *Process Saf. Environ. Prot.* **2019**, *125*, 342–357. [CrossRef]
65. Gilbert, J.J.; Ray, S.; Das, D. Hydrogen production using Rhodobacter sphaeroides (O.U. 001) in a flat panel rocking photobioreactor. *Int. J. Hydrogen Energy* **2011**, *36*, 3434–3441. [CrossRef]
66. Rodríguez-Reyes, J.J.; García-Depraect, O.; Cantera, S.; Mena-Navarro, V.; León-Becerril, E. Assessment of the recovery of hydrogen production activity in dark fermentation reactors after a long period of shutdown. *Int. J. Hydrogen Energy* **2025**, *144*, 1134–1146. [CrossRef]
67. Clark, I.C.; Zhang, R.H.; Upadhyaya, S.K. The effect of low pressure and mixing on biological hydrogen production via anaerobic fermentation. *Int. J. Hydrogen Energy* **2012**, *37*, 11504–11513. [CrossRef]
68. Song, Z.; Dai, Y.; Fan, Q.; Li, X.; Fan, Y.; Hou, H. Effects of pretreatment method of natural bacteria source on microbial community and bio-hydrogen production by dark fermentation. *Int. J. Hydrogen Energy* **2012**, *37*, 5631–5636. [CrossRef]
69. Dreschke, G.; Papirio, S.; Lens, P.N.L.; Esposito, G. Influence of liquid-phase hydrogen on dark fermentation by Thermotoga neapolitana. *Renew. Energy* **2019**, *140*, 354–360. [CrossRef]
70. Ananthi, V.; Bora, A.; Ramesh, U.; Yuvakkumar, R.; Raja, K.; Ponnuchamy, K.; Muthusamy, G.; Arun, A. A review on the technologies for sustainable biohydrogen production. *Process Saf. Environ.* **2024**, *186*, 944–956. [CrossRef]
71. Sekoai, P.T.; Yoro, K.O.; Daramola, M.O. Effect of nitrogen gas sparging on dark fermentative biohydrogen production using suspended and immobilized cells of anaerobic mixed bacteria from potato waste. *Biofuels* **2018**, *9*, 595–604. [CrossRef]
72. Winkler, J.; Neuner, T.; Hupfauf, S.; Arthofer, A.; Ebner, C.; Rauch, W.; Bockreis, A. Impact of impeller design on anaerobic digestion: Assessment of mixing dynamics, methane yield, microbial communities and digestate dewaterability. *Bioresour. Technol.* **2024**, *406*, 131095. [CrossRef] [PubMed]
73. Clagnan, E.; Adani, F. Influence of feedstock source on the development of polyhydroxyalkanoates-producing mixed microbial cultures in continuously stirred tank reactors. *New Biotechnol.* **2023**, *76*, 90–97. [CrossRef] [PubMed]
74. Arslan, D.; Steinbusch, K.J.J.; Diels, L.; De Wever, H.; Hamelers, H.V.M.; Buisman, C.J.N. Selective carboxylate production by controlling hydrogen, carbon dioxide and substrate concentrations in mixed culture fermentation. *Bioresour. Technol.* **2013**, *136*, 452–460. [CrossRef] [PubMed]
75. Feng, K.; Wang, Q.; Li, H.; Zhang, Y.; Deng, Z.; Liu, J.; Du, X. Effect of fermentation type regulation using alkaline addition on two-phase anaerobic digestion of food waste at different organic load rates. *Renew. Energy* **2020**, *154*, 385–393. [CrossRef]
76. Dahiya, S.; Mohan, S.V. Selective control of volatile fatty acids production from food waste by regulating biosystem buffering: A comprehensive study. *Chem. Eng. J.* **2019**, *357*, 787–801. [CrossRef]
77. Zhu, X.; Leininger, A.; Jassby, D.; Tsesmetzis, N.; Ren, Z.J. Will membranes break barriers on volatile fatty acid recovery from anaerobic digestion? *ACS EST Eng.* **2021**, *1*, 141–153. [CrossRef]
78. Liu, G.; Lu, H.; Wu, K.; Guan, G.; Liang, B. Co-production of high-purity hydrogen and value-added molecules from cellulose under alkaline environment: Mechanism and application. *Renew. Energy* **2025**, *252*, 123472. [CrossRef]
79. Song, S.; Ginige, M.P.; Yu Cheng, K.; Peacock, C.S.; Kaksonen, A.H. Ultrasonication-induced metabolic pathway shifts and reduced electron carrier washout with biomass enhanced hydrogen yield in a continuous stirred tank reactor. *Chem. Eng. J.* **2024**, *493*, 152594. [CrossRef]
80. Oshiki, M.; Yamaguchi, G.; Takahashi, K.; Okabe, S.; Kawano, S.; Nakagawa, J.; Fukushima, T. Thermophilic dark fermentation for hydrogen and volatile fatty acids production from breadcrumbs. *Chem. Eng. J.* **2024**, *501*, 157633. [CrossRef]
81. Naccache, G.; Paraschivoiu, M. Parametric study of the dual vertical axis wind turbine using CFD. *J. Wind. Eng. Ind. Aerod.* **2018**, *172*, 244–255. [CrossRef]
82. Mokhtarani, B.; Zanganeh, J.; Moghtaderi, B. A Review on Biohydrogen Production Through Dark Fermentation, Process Parameters and Simulation. *Energies* **2025**, *18*, 1092. [CrossRef]
83. Meersseman Arango, H.; Luis, P.; Leyssens, T.; Debecker, D.P. Enzyme-membrane reactors: Recent trends and applications for the production of fine chemicals and pharmaceutical building blocks. *Comptes Rendus Chim.* **2025**, *28*, 151–170. [CrossRef]
84. Renaudie, M.; Clion, V.; Dumas, C.; Vuilleumier, S.; Ernst, B. Intensification and optimization of continuous hydrogen production by dark fermentation in a new design liquid/gas hollow fiber membrane bioreactor. *Chem. Eng. J.* **2021**, *416*, 129068. [CrossRef]
85. Bérubé, P.R.; Lei, E. The effect of hydrodynamic conditions and system configurations on the permeate flux in a submerged hollow fiber membrane system. *J. Membrane Sci.* **2006**, *271*, 29–37. [CrossRef]
86. Zhang, K.; Cui, Z.; Field, R.W. Effect of bubble size and frequency on mass transfer in flat sheet MBR. *J. Membrane Sci.* **2009**, *332*, 30–37. [CrossRef]

87. Sun, J.; Zhang, X.; Guan, J.; He, Z. Volatile Fatty Acid Production through Arresting Methanogenesis by Electro-Synthesized Hydrogen Peroxide in Anaerobic Digestion and Subsequent Recovery by Electrodialysis. *ACS ES T Eng.* **2024**, *4*, 2964–2973. [CrossRef]
88. Show, K.Y.; Lee, D.J.; Tay, J.H.; Lin, C.Y.; Chang, J.S. Biohydrogen production: Current perspectives and the way forward. *Int. J. Hydrogen Energy* **2012**, *37*, 15616–15631. [CrossRef]
89. Jiang, Y.; Xu, W.; Zhang, Y.; Yan, R.; Xie, Y.; Zhang, D.; Jia, F.; Yang, L.; Zaib, S.; Li, R.; et al. Effectiveness and mechanism of using sodium alginate-magnesium silicate carrier in UASB reactor to resist shock loading of coking wastewater. *J. Clean. Prod.* **2025**, *506*, 145519. [CrossRef]
90. Afridi, Z.U.R.; Wu, J.; Li, Z.H.; Akand, R.; Cao, Z.P.; Poncin, S.; Li, H.Z. Novel insight of spatial mass transfer conditions of upflow anaerobic reactor. *J. Clean. Prod.* **2018**, *204*, 390–398. [CrossRef]
91. Łukajtis, R.; Hołowacz, I.; Kucharska, K.; Glinka, M.; Rybarczyk, P.; Przyjazny, A.; Kamiński, M. Corrigendum to "Hydrogen production from biomass using dark fermentation" [Renew Sustain Energy Rev 91 (2018) 665–94]. *Renew. Sustain. Energy Rev.* **2018**, *95*, 354. [CrossRef]
92. Tugtas, A.E.; Yesil, H.; Calli, B. Enhanced anaerobic digestion model no.1 for high solids fermentation: Integrating homoacetogenesis and chain elongation. *Bioresour. Technol.* **2025**, *417*, 131843. [CrossRef] [PubMed]
93. Chen, H.; Fu, Y.; Song, Y.; Wu, Q.; Cao, W.; Liu, Z.; Wei, X. Study on the process and performance of anaerobic circulating fluidized bed: Effects of fluidization velocity and particle circulation rate on hydrogen production. *Int. J. Hydrogen Energy* **2024**, *91*, 343–353. [CrossRef]
94. Encina, P.A.G.; Hidalgo, M.D. Influence of substrate feed patterns on biofilm development in anaerobic fluidized bed reactors (AFBR). *Process Biochem.* **2005**, *40*, 2509–2516. [CrossRef]
95. Han, W.; Hu, Y.; Li, S.; Nie, Q.; Zhao, H.; Tang, J. Effect of organic loading rate on dark fermentative hydrogen production in the continuous stirred tank reactor and continuous mixed immobilized sludge reactor from waste pastry hydrolysate. *Waste Manag.* **2016**, *58*, 335–340. [CrossRef] [PubMed]
96. Martínez-Mendoza, L.J.; García-Depraect, O.; Muñoz, R. Unlocking the high-rate continuous performance of fermentative hydrogen bioproduction from fruit and vegetable residues by modulating hydraulic retention time. *Bioresour. Technol.* **2023**, *373*, 128716. [CrossRef] [PubMed]
97. Saleem, M.; Lavagnolo, M.C.; Spagni, A. Biological hydrogen production via dark fermentation by using a side-stream dynamic membrane bioreactor: Effect of substrate concentration. *Chem. Eng. J.* **2018**, *349*, 719–727. [CrossRef]
98. Sivagurunathan, P.; Anburajan, P.; Kumar, G.; Kim, S. Effect of hydraulic retention time (HRT) on biohydrogen production from galactose in an up-flow anaerobic sludge blanket reactor. *Int. J. Hydrogen Energy* **2016**, *41*, 21670–21677. [CrossRef]
99. Mahmod, S.S.; Azahar, A.M.; Tan, J.P.; Jahim, J.M.; Abdul, P.M.; Mastar, M.S.; Anuar, N.; Mohammed Yunus, M.F.; Asis, A.J.; Wu, S. Operation performance of up-flow anaerobic sludge blanket (UASB) bioreactor for biohydrogen production by self-granulated sludge using pre-treated palm oil mill effluent (POME) as carbon source. *Renew. Energy* **2019**, *134*, 1262–1272. [CrossRef]
100. Rydén, M.; Arjmand, M. Continuous hydrogen production via the steam–iron reaction by chemical looping in a circulating fluidized-bed reactor. *Int. J. Hydrogen Energy* **2012**, *37*, 4843–4854. [CrossRef]
101. Park, S.; Rhee, C.; Jadhav, D.A.; Jang, J.; Hwang, M.; Chae, K. Enhanced hydrogen production in microbial electrolysis cells through a magnetically induced electroactive anode biofilm. *Chem. Eng. J.* **2025**, *505*, 159071. [CrossRef]
102. Guerrero-Sodric, O.; Baeza, J.A.; Guisasola, A. Enhancing bioelectrochemical hydrogen production from industrial wastewater using Ni-foam cathodes in a microbial electrolysis cell pilot plant. *Water Res.* **2024**, *256*, 121616. [CrossRef] [PubMed]
103. Yang, M.; Luo, S.; Yuan, R.; Hou, R.; Zhou, B.; Chen, H. Cathode materials and novel strategies for improving bioenergy production in microbial electrolysis cell: A review. *J. Environ. Chem. Eng.* **2025**, *13*, 115718. [CrossRef]
104. Lee, H.; Xin, W.; Katakojwala, R.; Venkata Mohan, S.; Tabish, N.M.D. Microbial electrolysis cells for the production of biohydrogen in dark fermentation—A review. *Bioresour. Technol.* **2022**, *363*, 127934. [CrossRef] [PubMed]
105. Chookaew, T.; Prasertsan, P.; Ren, Z.J. Two-stage conversion of crude glycerol to energy using dark fermentation linked with microbial fuel cell or microbial electrolysis cell. *New Biotechnol.* **2014**, *31*, 179–184. [CrossRef] [PubMed]
106. Chaitanya, N.K.; Rajpurohit, A.; Nair, P.S.; Chatterjee, P. Enhanced carbon capture and medium chain fatty acid production using microbial electrosynthesis: Role of electrode surface area. *Bioresour. Technol.* **2025**, *435*, 132916. [CrossRef] [PubMed]
107. Bian, B.; Bajracharya, S.; Xu, J.; Pant, D.; Saikaly, P.E. Microbial electrosynthesis from CO_2: Challenges, opportunities and perspectives in the context of circular bioeconomy. *Bioresour. Technol.* **2020**, *302*, 122863. [CrossRef] [PubMed]
108. Lim, S.S.; Kim, B.H.; Li, D.; Feng, Y.; Daud, W.R.W.; Scott, K.; Yu, E.H. Effects of applied potential and reactants to hydrogen-producing biocathode in a aicrobial electrolysis Ccell. *Front. Chem.* **2018**, *6*, 318. [CrossRef] [PubMed]
109. Bian, Y.; Leininger, A.; May, H.D.; Ren, Z.J. H_2 mediated mixed culture microbial electrosynthesis for high titer acetate production from CO_2. *Environ. Sci. Ecotechnol.* **2024**, *19*, 100324. [CrossRef] [PubMed]
110. Thulluru, L.P.; Dhanda, A.; Doki, M.M.; Ghangrekar, M.M.; Chowdhury, S. Sludge-derived hydrochar as a potential electrocatalyst for improved CO_2 reduction in microbial electrosynthesis. *RSC Sustain.* **2025**, *3*, 471–485. [CrossRef]

111. Yao, H.; Romans-Casas, M.; Vassilev, I.; Rinta-Kanto, J.M.; Puig, S.; Rissanen, A.J.; Kokko, M. Selective butyrate production from CO_2 and methanol in microbial electrosynthesis—Influence of pH. *Bioelectrochemistry* **2025**, *165*, 109000. [CrossRef] [PubMed]
112. Varghese, V.K.; Poddar, B.J.; Shah, M.P.; Purohit, H.J.; Khardenavis, A.A. A comprehensive review on current status and future perspectives of microbial volatile fatty acids production as platform chemicals. *Sci. Total Environ.* **2022**, *815*, 152500. [CrossRef] [PubMed]

Disclaimer/Publisher's Note: The statements, opinions and data contained in all publications are solely those of the individual author(s) and contributor(s) and not of MDPI and/or the editor(s). MDPI and/or the editor(s) disclaim responsibility for any injury to people or property resulting from any ideas, methods, instructions or products referred to in the content.